© 2022. Published by The Company of Biologists Ltd | Journal of Experimental Biology (2022) 225, jeb243498. doi:10.1242/jeb.243498

RESEARCH ARTICLE

Knifefish turning control and hydrodynamics during forward swimming

Olivia H. Hawkins[1,2,*], Víctor M. Ortega-Jiménez[3] and Christopher P. Sanford[4]

ABSTRACT

Rapid turning and swimming contribute to ecologically important behaviors in fishes such as predator avoidance, prey capture, mating and the navigation of complex environments. For riverine species, such as knifefishes, turning behaviors may also be important for navigating locomotive perturbations caused by turbulent flows. Most research on fish maneuvering focuses on fish with traditional fin and body morphologies, which primarily use body bending and the pectoral fins during turning. However, it is uncertain how fishes with uncommon morphologies are able to achieve sudden and controllable turns. Here, we studied the turning performance and the turning hydrodynamics of the black ghost knifefish (*Apteronotus albifrons*, *N*=6) which has an atypical elongated ribbon fin. Fish were filmed while swimming forward at ∼2 body lengths s^{-1} and feeding from a fixed feeder (control) and an oscillating feeder (75 Hz) at two different amplitudes. 3D kinematic analysis of the body revealed the highest pitch angles and lowest body bending coefficients during steady swimming. Low pitch angle, high maximum yaw angles and large body bending coefficients were characteristic of small and large turns. Asynchrony in pectoral fin use was low during turning; however, ribbon fin wavelength, frequency and wave speed were greatest during large turns. Digital particle image velocimetry (DPIV) showed larger counter-rotating vortex pairs produced during turning by the ribbon fin in comparison to vortices rotating in the same direction during steady swimming. Our results highlight the ribbon fin's role in controlled rapid turning through modulation of wavelength, frequency and wave speed.

KEY WORDS: Fish locomotion, Swimming control, Maneuverability, Ribbon fin

INTRODUCTION

Turning maneuvers are commonly used by fishes during prey capture, predator avoidance, mating or navigation of complex environments (Webb, 1981). Turning during prey capture is especially important when pursuing evasive prey items (Domenici, 2001). For instance, after shooting prey with a jet of water, banded archer fish (*Toxotes jaculatrix*) turn rapidly to face and approach the quickly falling prey (Wöhl and Schuster, 2007). Larval zebrafish (*Brachydanio rerio*) rely on routine turning maneuvers to approach and capture prey, but also produce quick large-angle turns as a form of an escape response when presented with a stimulus (Budick and O'Malley, 2000). Escape responses in the context of predator avoidance have been studied in many groups of fishes including sharks, bichirs, larval fishes, trout and sunfishes, and have direct fitness consequences (Webb, 1976, 1978; Budick and O'Malley, 2000; Tytell and Lauder, 2002; Domenici et al., 2004; Gibb et al., 2006; Tytell and Lauder, 2008). An additional context in which turning has direct fitness consequences is during mating events. Some fishes perform rapid turns during courting behavior, such as the round belly cowfish (*Lactoria diaphanus*) in which the males rapidly and continually swim circles around the female, which also turns to follow the male or flees (Moyer, 1979). Mating displays in high-backed pygmy swordtails (*Xiphophorus multilineatus*) also rely on turns in order for the male to showcase the vertical body bars on each side of its body to the female (Liotta et al., 2019). Finally, turning in the context of habitat navigation is shown to be especially important for fishes living in complex environments such as coral reefs (Gerstner, 1999). In freshwater systems, littoral ecomorphs of bluegill sunfish (*Lepomis macrochirus*), which live amongst dense vegetation, have better performance while navigating an obstacle course in comparison with pelagic ecomorphs (Ellerby and Gerry, 2011). While turning is an important maneuver throughout a fish's life, there are still many species for which investigations of turning performance and kinematics are limited.

Most of what we know about the kinematics and hydrodynamics of routine turning maneuvers comes from fishes such as sunfish and trout that use the body and caudal fin to power steady swimming (Drucker and Lauder, 2001, 2002; Lauder and Drucker, 2004). For these body undulating fishes, large normal forces produced by the body and caudal fin increase the momentum around the fish's center of mass, thus aiding in turning maneuvers (Weihs, 1972). In addition to these surfaces, the median fins also play a role in turning in fishes. In bluegill sunfish, the dorsal and anal fins contribute part of the momentum needed to complete turns (Lauder and Drucker, 2004; Standen and Lauder, 2005; Tytell and Lauder, 2008). In brook trout (*Salvelinus fontinalis*), the anal fin plays more of a role in additive force generation with the caudal fin as the dorsal fin is more anterior (Standen and Lauder, 2007). Furthermore, brook trout use their pelvic fins to stabilize the body after turning (Standen, 2008). Similar to bluegill, bluefin tuna (*Thunnus thynnus)* and yellowfin tuna (*Thunnus albacares*) use the dorsal and anal fins to power turns in which the anterior dorsal fin is recruited for powering the turns and the posterior dorsal and anal fin are used to stabilize the body during the turn (Pavlov et al., 2017; Feng et al., 2020; Li, 2021). In addition to forces produced by the body, median and caudal fins, turning in sunfishes and trout is partly powered by imbalanced forces generated from asynchronous movements of the pectoral fins (Drucker and Lauder, 2002; Lauder and Drucker,

[1]Department of Ecology, Evolution and Organismal Biology, Kennesaw State University, Kennesaw, GA 30144, USA. [2]Department of Biology, University of Louisiana at Lafayette, Lafayette, LA 70503, USA. [3]School of Chemical and Biomolecular Engineering, Georgia Institute of Technology, Atlanta, GA 30332, USA. [4]Research and Sponsored Programs, California State University, Northridge, CA 91330, USA.

*Author for correspondence (ohawkins.research@gmail.com)

O.H.H., 0000-0001-9373-5919; Víctor M.O., 0000-0003-0024-5086; C.P.S., 0000-0003-1876-9910

Received 10 September 2021; Accepted 22 February 2022

2004). In bluegill sunfish specifically, the pectoral fins are integral to maneuvering through complex environments even in the absence of traditional sensory cues (Flammang and Lauder, 2013). In fishes with rigid bodies, such as the spotted boxfish (*Ostracion meleagris*), the pectoral fins are the primary control surfaces used for turning (Walker, 2000). Overall, body bending and the pectoral fins are the most commonly used surfaces for most bony fishes during turning maneuvers (Drucker and Lauder, 2001, 2002).

While many fishes use body bending and the pectoral fins to turn, it is not known how fishes with uncommon fin morphologies perform turning maneuvers with a non-traditional control surface such as the ribbon fin. The ribbon fin is present in multiple groups of fishes and can be found in dorsal, ventral or dorso-ventral positions, driving swimming by producing waves without body bending. Representatives of ribbon fin locomotion exist in multiple orders of both freshwater and marine fishes (Jagnandan and Sanford, 2013). Although the selective pressure on the evolution of ribbon finned fishes remains unknown, it has been suggested that swimming with an undulatory fin reduces mechanical and energetic costs while increasing maneuverability (Blake, 1983; Shirgaonkar et al., 2008; Neveln et al., 2013). Despite the implications of this fin for enhanced maneuverability, no study has investigated turning performance in a fish with a ribbon fin. This is surprising given that most ribbon fin swimmers live in structurally and hydrodynamically complex habitats (e.g. coral reefs, vegetated streams).

One commonly studied ribbon fin swimmer is the weakly electric black ghost knifefish, *Apteronotus albifrons*. *Apteronotus albifrons* is one of 170 species of knifefish that swim using the gymnotiform mode (ventral ribbon fin propulsion) and inhabits the floodplains of the Amazon River which are dominated by heavy vegetation, macrophyte stems and flooded forests (Crampton, 1996; Albert, 2001; Albert and Crampton, 2005). The extensive vegetation of these floodplains provides structural obstacles that increase habitat complexity and also cause complex flow patterns that can impact swimming performance (Ortega-Jimenez and Sanford, 2021). Beyond habitat navigation, turning also impacts foraging success. Apteronotids forage for small and active prey such as *Daphnia*, which require them to maneuver rapidly in order to feed (Nelson and MacIver, 1999). As the ecology *A. albifrons* is not well understood, investigations focusing on maneuvering performance have implications for understanding constraints on habitat navigation and foraging in the presence of unpredictable flooding and drought conditions in the Amazon due to climate change (Katz et al., 2020).

To date, most research on the locomotion performance of *A. albifrons* has focused on steady swimming (Shirgaonkar et al., 2008; Ruiz-Torres et al., 2013; Youngerman et al., 2014). Under laminar flow conditions, *A. albifrons* uses the ribbon fin to move linearly while maintaining a rigid body, therefore reducing potential disruption to its electrosensory system during prey detection (MacIver et al., 2010). Given the mechanical efficiency of ribbon fin locomotion, many studies have investigated steady swimming maneuvers computationally and through bioinspired automated underwater vehicles (AUVs) (MacIver et al., 2004; Shirgaonkar et al., 2008; Curet et al., 2011; Neveln et al., 2013; Liu and Curet, 2018; English et al., 2019). All of these studies highlight how modulation of various parameters of the ribbon fin (i.e. curvature, frequency, wavelength) impact forward swimming speed, backwards swimming and hovering without consideration of the potential impact of traditional control surfaces such as the body and the pectoral fins. A recent study demonstrated that *A. albifrons* uses a combination of the body, pectoral fins and the ribbon fin to navigate through unsteady flows (Ortega-Jimenez and Sanford, 2021). However, the contribution of these different control surfaces to turning maneuvers in steady flows, especially the ribbon fin, remains largely unexplored. Therefore, this study investigated the turning performance of *A. albifrons*, a fish with a non-traditional control surface, and its associated hydrodynamics. We used 3D kinematics to assess the contribution of the body, pectoral fins and ribbon fin to steady swimming, small turns and large turns while swimming forward. We also characterized the fluid dynamics of the wake produced by the ribbon fin during each maneuver. We predicted that the ribbon fin would contribute most to steady swimming, pectoral fins would dominate small turns, and that large turns would rely on all three control surfaces. This study specifically investigated the important role of the ribbon fin in eliciting small and large turns during forward swimming.

MATERIALS AND METHODS

Animal care and training

Six juvenile black ghost knifefish (*Apteronotus albifrons* Linneaus 1766; 10.2±0.86 cm) were obtained from local suppliers in Kennesaw, GA, USA. Fish were housed separately in 151 liter tanks containing dechlorinated freshwater. All tanks were maintained at 25–26°C, pH 7–8. The aquatics facility maintained a 12 h:12 h light:dark photoperiod. Fish received bloodworms *ad libitum*.

Prior to experiments, fish were trained to approach and follow an oscillating feeder under low flow conditions [~2 body lengths (BL) s^{-1}; see 'Experimental design']. We used an oscillating feeder to establish three standardized treatments: steady forward swimming, small turns and large turns. Fish received a week of training for all three treatments. For further details on training, see Ortega-Jimenez and Sanford (2021). Food was withheld 24 h before experiments, and fish received a 30 min acclimation period before filming. All fish performed all three treatments, and treatment order was assigned at random. Husbandry and experiments adhered to Kennesaw State University IACUC (ACUP# 20-008) and followed federal guidelines and regulations. No fish were killed for the purposes of this study.

Experimental design

Fish were filmed in a Brett-type 90 liter recirculating flow tank (Loligo Systems, Swim-90, Tjele, Denmark) with dechlorinated freshwater maintained at 25–26°C. We used a single flow speed (15 cm s^{-1}, ~2 BL s^{-1}) to encourage forward swimming (Ortega-Jimenez and Sanford, 2021). The feeder (16 cm) was centered in the working section 8 cm from the bottom (70×20×20 cm; Fig. 1). We used the custom-built oscillating feeder to differentiate between treatments. It consisted of a feeding tube attached to the control arm of a waterproof 20 kg digital servo motor programmed by an Arduino Uno R3 microcontroller (Fig. 1). The feeding tube was composed of a small plastic cylinder with a 1 mm diameter hole in the center to hold bloodworms as described in Ortega-Jimenez and Sanford (2021). During steady swimming, the feeder remained stationary in the center of the working section. For the turning treatments, the feeder was programmed to oscillate at identical frequencies (0.75 Hz) but different angular amplitudes (30 and 45 deg, respectively). For small turn treatments, one full oscillation of the feeder occurred over a horizontal distance of 8 cm at an average speed of 3.1 cm s^{-1}. For large turn treatments, one full oscillation covered a horizontal distance of 14 cm at an average speed of 4.7 cm s^{-1}.

Journal of Experimental Biology (2022) 225, jeb243498. doi:10.1242/jeb.243498

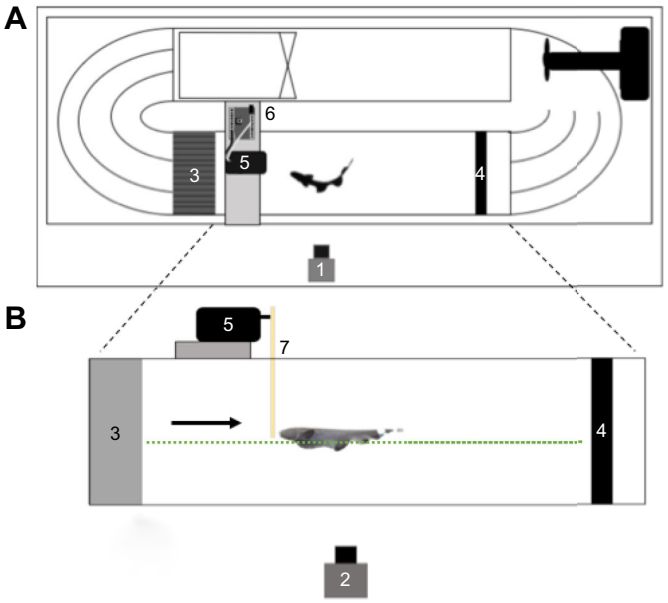

Fig. 1. Experimental set-up. Experimental set-up of the flow tank including the aerial view (A) and lateral view (B). Cameras were placed lateral (1) and ventral (2) to the working section of the flow tank. A flow rectifier (3) and mesh (4) were placed upstream and downstream of the working section, respectively. The oscillating feeder was placed in the center of the working section and consisted of a digital servo motor (5) programed by an Arduino Uno R3 microcontroller (6) with an attached feeder (7). The black arrow indicates the direction of flow (in body lengths s^{-1}, BL s^{-1}), and the green dotted line shows the location of the laser sheet used for digital particle image velocimetry (DPIV). Schematic diagram not drawn to scale.

Filming and digitization

We filmed at 250 frames s^{-1} using two synchronized Hi-Spec4 cameras (1696×1710 pixels; Fastec Imaging, San Diego, CA, USA). Cameras were placed lateral and ventral to the working section (Fig. 1). Cameras were calibrated using a 24-point calibration cube and the direct linear transfer method (DLT, version 7.1: Hedrick, 2008) for Matlab (Matlab 2020b, MathWorks, Natick, MA, USA). Sequences in which the fish swam for ∼8 s behind the feeder or completed a full turn to either the left or the right were retained for analysis. DLT software was also used to track the movement of the body, pectoral fins and ribbon fin during steady swimming and turning using 14 digitized landmarks. Calibration and digitization code is available from: http://biomech.web.unc.edu/dltdv/. Representative video sequences of each treatment can be viewed in Movie 1.

Body landmarks were placed on the tip the of the snout, in between the pectoral fins, behind the pectoral fins, in the middle of the body, at the end of the ribbon fin attachment and at the tip of the caudal fin. Pectoral fin landmarks were placed on the tip of the most distal fin ray and at the base of the fins. Ribbon fin landmarks were placed at the base of a fin ray at the center of the ribbon fin, on the distal end of the same fin ray, and on the tip of a distal fin ray located on the following wave crest. For additional information on landmarks, see Fig. 2.

Kinematic measurements

For steady swimming, we analyzed sequences in which the fish had already approached the feeder and where the ribbon fin undulated for at least two cycles (N=6, 5–7 sequences per fish). For the small turn and large turn treatments, we analyzed sequences where the fish made a full turn to either the right or the left which was half of the total oscillation distance (small turn: N=6, 6–9 sequences per fish; large turn: N=6, 5–8 sequences per fish). The number of sequences analyzed for each individual for each treatment is given in Table S1. Kinematic variables detailed below were averaged for each fish and then averaged across all fish per treatment.

Variables of interest for the body consisted of pitch angle (deg), maximum yaw angle (deg) and the body bending coefficient (β_b). Pitch angle was calculated as the angular orientation of the body with reference to a horizontal plane. A positive pitch angle indicated a head-up orientation of the body while a negative pitch angle indicated a head-down orientation. We calculated yaw angle as the angular displacement of the body in the horizontal plane. β_b, as described by Azizi and Landberg (2002), quantifies whole-body curvature. The coefficient is calculated as follows:

$$\beta_b = 1 - \frac{L_c}{L_b}, \quad (1)$$

in which the distance between the snout and the end of the caudal fin (L_c) is divided by total body length (L_b) and subtracted from 1 (Fig. 2).

For the pectoral fins, we quantified pectoral fin flapping frequency (Hz), the dorso-ventral pectoral abduction angle (deg), and the asynchronous index (AI). Pectoral flapping frequency and the dorso-ventral abduction angle were quantified using only the left pectoral fin as it was the only visible fin in both lateral and ventral views. Flapping frequency was calculated by tracking the tip of the left pectoral fin in the vertical plane throughout the sequence. The dorso-ventral abduction angle was quantified as the angle formed between the body and the tip of the left pectoral fin as it moved dorso-ventrally. The AI used in this study was adapted and modified from Gerry et al. (2008):

$$\mathrm{AI} = \frac{\sum \frac{X_{\mathrm{right}}}{|X_{\mathrm{right}}|} - \frac{X_{\mathrm{left}}}{|X_{\mathrm{left}}|}}{2(n_{\mathrm{frames}} - 1)}, \quad (2)$$

in which AI is the sum of the ratios of the consecutive difference in x positions of the right pectoral fin to the absolute value of the same positions minus the ratio of the difference in x positions of the left pectoral fin to the absolute value of those same positions, all divided by 2 times the number of frames (n_{frames}) analyzed minus 1. This index is used to determine the percentage of the time the pectoral fins are moving in the same direction (synchronously) or different directions (asynchronously). AI values closer to one indicate the fins are moving more asynchronously while values closer to 0 suggest less asynchronous movements of the fins.

Variables of interest for the ribbon fin included ribbon fin amplitude (deg), frequency (Hz), wavelength (cm) and wave speed (cm s^{-1}). We defined amplitude as the stroke angle followed by the base and distal tip of a central fin ray, while frequency was the inverse period of the wave determined by the same two landmarks. We calculated wavelength as the distance between the tips of two consecutive wave crests. Wave speed was determined using the movement of a landmark at the distal tip of the fin ray at the middle of a wave crest and calculating the resulting first derivative of the mean square error (MSE)-quintic spline function (Walker, 1998; Ortega-Jimenez and Sanford, 2021). The MSE-quintic spline function smooths kinematic displacement data to reduce possible noise from digitization when calculating velocity and acceleration (Zin et al., 2020). See Ortega-Jimenez and Sanford (2021) for further details on the quantification of the ribbon fin variables.

Journal of Experimental Biology (2022) 225, jeb243498. doi:10.1242/jeb.243498

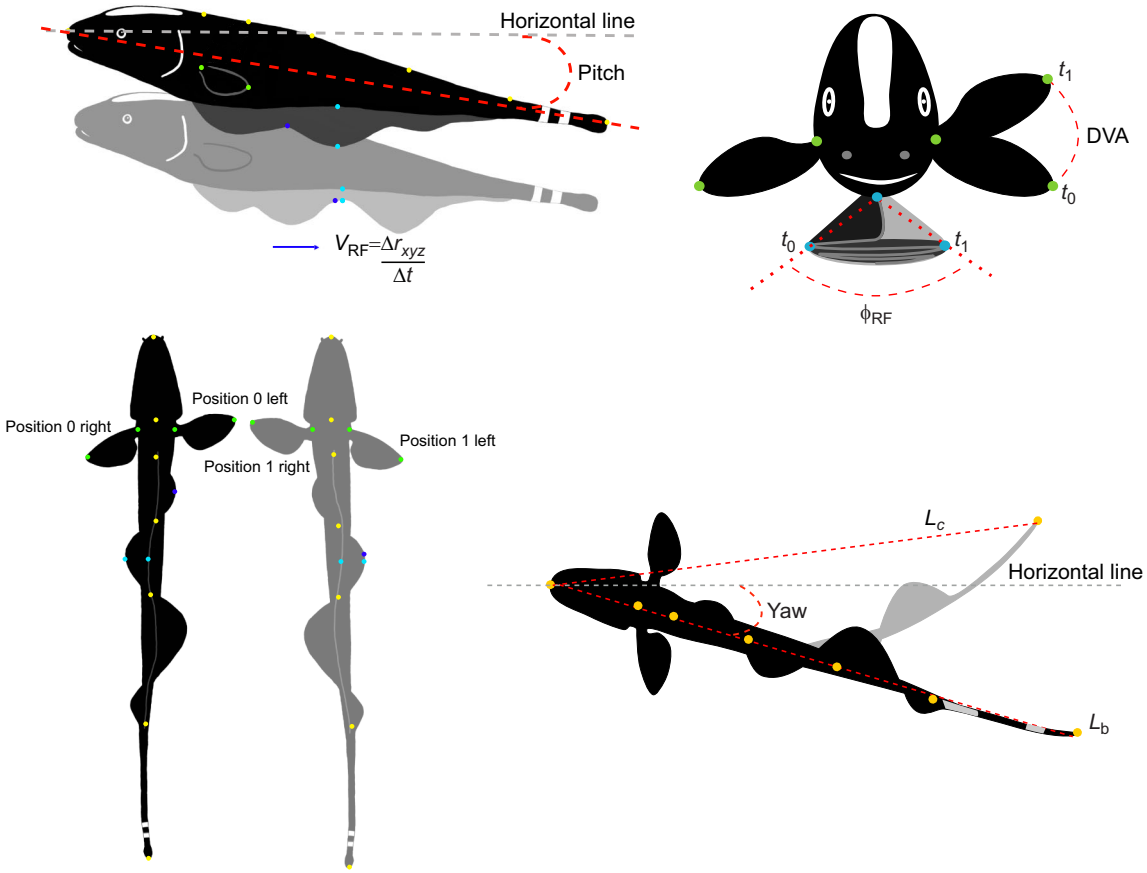

Fig. 2. Digitization landmarks. Schematic diagram of the 14 digitized landmarks used in the calculation of pitch angle, maximum yaw angle, body bending coefficient, dorso-ventral pectoral fin abduction angle (DVA), asynchronous index (AI), pectoral fin flapping frequency, ribbon fin amplitude, ribbon fin wavelength and ribbon fin wave speed. Yellow dots represent body points, green dots represent pectoral fin points, light blue dots represent fixed ribbon fin points, and the dark blue dot represents a moving ribbon fin point. See Materials and Methods, 'Filming and digitization' and 'Kinematic measurements' for detailed information on each variable. V_{RF}, ribbon fin wave speed; Δr_{xyz}, change in 3D position of ribbon fin landmark; Δt, temporal series of landmarks; RF, ribbon fin; t_0, time 0 (beginning digitization); t_1, time 1 (next digitization landmark); ϕ_{RF}, ribbon fin wave amplitude; L_c, distance between the snout and the end of the caudal fin; L_b, total body length. Figure reproduced and modified from Ortega-Jimenez and Sanford (2021).

Digital particle image velocimetry (DPIV) and analysis

Plastic particles (50 µm) were illuminated using a class-4 laser (Opto Engine LLC, Midvale, UT, USA; 532 nm, 5 W). The horizontal laser sheet was oriented approximately 1 cm below the oscillating feeder. Sequences were filmed at 500 frames s^{-1} with a HiSpec 4 camera placed ventral to the working section of the flow tank (Fig. 1B). Two fish were used for DPIV analysis, and we filmed both fish performing all three treatments at a flow speed of 15 cm s^{-1} (~2 BL s^{-1}). Sequences in which only the ribbon fin intersected the laser sheet were kept for analysis. We used PIVlab version 2.50 in Matlab for the analysis of time-resolved paired images (Thielicke and Stamhuis, 2014). Interrogation windows of 64 $pixels^2$ to 32 $pixels^2$ (50% step) were applied to all sequences and removed any vectors with standard deviations over 5. The resulting vorticity fields during the turning treatments were visually characterized and compared among steady swimming, small turn and large turn treatments. We quantified the average vortex area for vortex pairs in each treatment using the 'Area Size' tool in PIVlab. Average vortex area (mm^2) consisted of values from both fish (steady swimming: n=14, small turn: n=22, large turn: n=14).

Statistical analysis

We used repeated measures ANOVA to determine the effect of treatment on the kinematic variables. For this analysis, we used the average values from each fish for each treatment. The Bonferroni pairwise comparison test served as *post hoc* analysis to assess significant differences between average values of the kinematic variables for steady swimming, small turns and large turns. Normality assumptions were visually confirmed using *Q*–*Q* plots. As we used a repeated measures design, we needed to verify that differences in the variation within-subjects among all possible combinations of the treatments remained equal. To test this assumption, we used Mauchly's test of sphericity, which assumes that variation is equal when α>0.05, and no violations of sphericity were detected. All data are presented as means±s.e.m.; means±s.d. are available in Table S2.

We used canonical discriminant analysis (CDA) as a multivariate approach to understand the contribution of the different body, pectoral fin and ribbon fin variables to each of the investigated maneuvers following the approach of Youngerman et al. (2014). For this analysis, all observations for each fish for each treatment were used. We excluded the dorso-ventral pectoral abduction angle from analysis because of its inability to meet the homogeneity of covariance assumption. After visually confirming multivariate normality through *Q*–*Q* plots, all other variables were kept in the model. We used Wilk's lambda to assess the discriminant axes significantly contributing to the maximum separation of the treatments (α=0.05). R version 4.1.1 was used for all statistical

Journal of Experimental Biology (2022) 225, jeb243498. doi:10.1242/jeb.243498

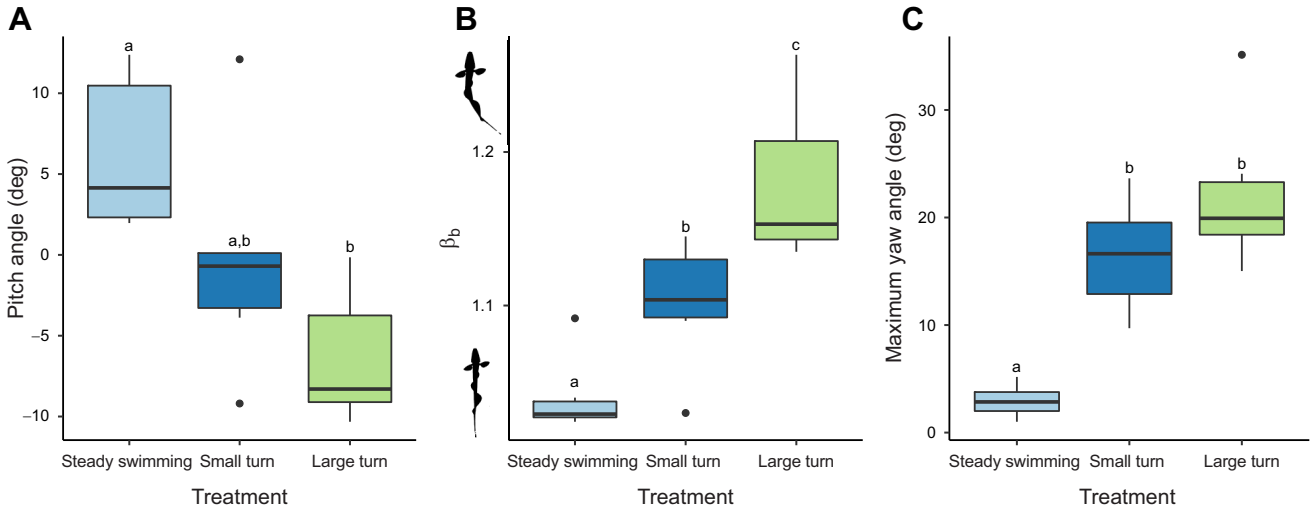

Fig. 3. Body kinematics results. Pitch angle (A), body bending coefficient β_b (B) and yaw angle (C) by treatment (n=6). Solid lines in the boxplots represent the median value of the variable while whiskers represent the minimum and maximum values. Letters indicate results of Bonferroni P-value adjustments following a one-way repeated measures ANOVA (α=0.05).

analyses including the candisc (https://CRAN.R-project.org/package=heplots), nlme (https://CRAN.R-project.org/package=nlme) and stats packages (http://www.R-project.org/).

RESULTS

Body kinematics

From steady swimming to large turns, the average pitch angle decreased significantly ($F_{2,10}$=6.45, P=0.02; Table S3; Fig. 3A). During steady swimming, the pitch angle was 6.16±2.00 deg, almost double the pitch angle of fish during large turns (−6.45±1.71 deg; Table 1). While pitch was significantly different between steady swimming and large turns (Bonferroni; t_5=3.78, P=0.04; Table 1), there were no significant differences in pitch angle between steady swimming and small turns, or between small and large turns (Bonferroni; t_5=1.64, P=0.49 and t_5=1.92, P=0.34, respectively; Table 1). Average β_b varied significantly across treatments ($F_{2,10}$=43.22, P<0.0001; Table S3; Fig. 3B). Significant differences in β_b were observed between steady swimming and large turns as well as between small and large turns (Bonferroni; t_5=−7.91, P<0.01 and t_5=−5.93, P<0.01, respectively; Table 1). β_b during steady swimming was significantly lower than that during small turns (Bonferroni; t_5=−4.43, P=0.02; Table 1). The average maximum yaw angle increased significantly across treatments ($F_{2,10}$=40.24, P<0.0001; Table S3; Fig. 3C). Maximum yaw angle during large turns was nearly 10 times that during steady swimming, but not significantly higher than that during small turns (Bonferroni; t_5=7.06, P=0.003 and t_5=0.05, P=0.15 respectively; Table 1).

Pectoral fin kinematics

Pectoral flapping frequency and dorso-ventral pectoral abduction angle were not found to significantly differ across treatments ($F_{2,10}$=0.36, P=0.71 and $F_{2,10}$=0.64, P=0.55, respectively; Table S3; Fig. 4A,B). The AI was found to differ significantly across treatments ($F_{2,10}$=7.87, P<0.01; Table S3; Fig. 4C). Average AI for the steady swimming treatment was 0.48±0.02 and was significantly larger than that during large turns (0.31±0.04; Bonferroni; t_5=4.69, P=0.02; Table 1). AI during steady swimming was higher than that for small turns but not significantly different (0.38±0.04; Bonferroni; t_5=1.86, P=0.37; Table 1). These results indicate that pectoral fins are moving asynchronously during all three treatments, but less asynchrony is occurring during large turns.

Ribbon fin kinematics

The average ribbon fin frequency differed significantly across treatments ($F_{2,10}$=5.35, P=0.03; Table S3; Fig. 5A). Ribbon fin frequency during large turns was significantly higher than that during small turns but not steady swimming (Bonferroni; t_5=−3.89, P=0.03 and t_5=−2.57, P=0.15, respectively; Table 1). Like ribbon

Table 1. Kinematic variables for the body, pectoral fins and ribbon fin

Kinematic variable	Steady swimming	Small turn	Large turn
Pitch angle (deg)	6.16±2.00^{a}	−0.38±2.87^{a,b}	−6.45±1.71^{b}
Maximum yaw angle (deg)	2.95±0.61^{a}	16.5±2.11^{b}	22.1±2.89^{b}
Body bending coefficient	1.04±0.01^{a}	1.10±0.02^{b}	1.17±0.02^{c}
Pectoral fin flapping frequency (Hz)	6.34±0.17^{a}	6.38±0.15^{a}	6.57±0.23^{a}
Dorso-ventral pectoral angle (deg)	43.95±2.15^{a}	39.35±3.30^{a}	42.37±1.89^{a}
Asynchronous index	0.48±0.02^{a}	0.38±0.04^{a,b}	0.31±0.04^{b}
Ribbon fin frequency (Hz)	6.62±0.14^{a,b}	6.64±0.25^{a}	7.56±0.26^{b}
Ribbon fin amplitude (deg)	78.52±6.34^{a}	68.85±3.08^{a}	64.98±6.55^{a}
Ribbon fin wavelength (cm)	0.43±0.11^{a}	0.86±0.15^{a,b}	1.11±0.10^{b}
Ribbon fin wave speed (cm s^{-1})	2.76±0.73^{a}	5.66±0.96^{b}	8.14±0.62^{b}

Results of kinematic measurements for each maneuver performed by *Apteronotus albifrons* (N=6). Results are reported here as means±s.e.m. using the means of all individuals during steady swimming, small turns and large turns. Superscript letters correspond to statistical significance among maneuvers determined by adjusted P-values from Bonferroni pairwise comparison tests following a one-way repeated measures ANOVA (α=0.05).

Journal of Experimental Biology (2022) 225, jeb243498. doi:10.1242/jeb.243498

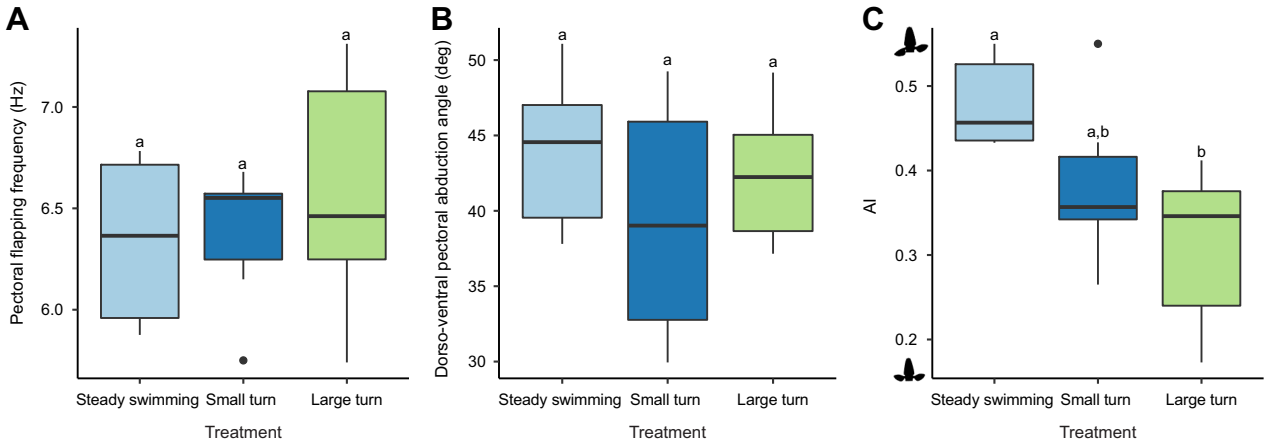

Fig. 4. Pectoral fin kinematics results. Pectoral fin flapping frequency (A), dorso-ventral pectoral abduction angle (B) and the AI (C) by treatment (n=6). Solid lines in the boxplots represent the median value of the variable while whiskers represent the minimum and maximum values. Letters indicate results of Bonferroni P-value adjustments following a one-way repeated measures ANOVA (α=0.05).

fin frequency, average wavelength differed significantly across treatments, increasing from steady swimming to large turns ($F_{2,10}$=7.84, P=0.009; Table S3; Fig. 5B). Wavelength during small turns was 0.86±0.15 cm, almost double the wavelength of the steady swimming treatment (Table 1). During large turns, the wavelength was significantly higher than that during steady swimming (Bonferroni; t_5=−3.76, P=0.04; Table 1).

Average ribbon fin amplitude decreased from steady swimming to large turns; however, treatment did not appear to have a significant effect ($F_{2,10}$=2.44, P=0.14; Table S3; Fig. 5C). Following in a similar pattern to ribbon fin frequency and wavelength, the average ribbon fin wave speed increased from steady swimming to large turns and differences were attributed to treatment ($F_{2,10}$=12.41, P<0.01; Table S3; Fig. 5D). Wave speed during small turns was significantly higher than that during steady swimming but not significantly lower than the wave speed during large turns (Bonferroni; t_5=−3.98, P=0.03 and t_5=−1.85, P=0.37, respectively; Table 1; Fig. 5D). Wave speed for large turns was 8.14

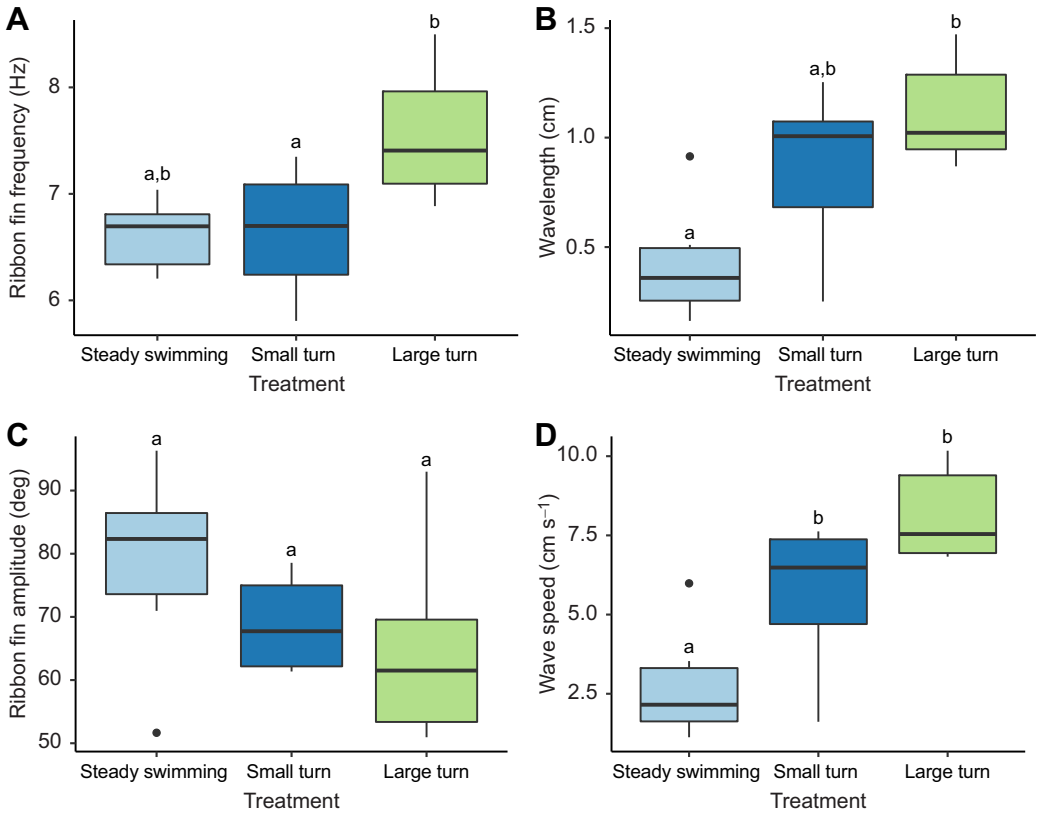

Fig. 5. Ribbon fin kinematics results. Ribbon fin frequency (A), wavelength (B), ribbon fin amplitude (C) and wave speed (D) by treatment (n=6). Solid lines in the boxplots represent the median value of the variable while whiskers represent the minimum and maximum values. Letters indicate results of Bonferroni P-value adjustments following a one-way repeated measures ANOVA (α=0.05).

Journal of Experimental Biology (2022) 225, jeb243498. doi:10.1242/jeb.243498

Table 2. Canonical discriminant analysis (CDA) axes results

Discriminant axis	Eigenvalue	Discriminant power (%)	Correlation	Wilk's lambda	*P*
1	3.03	97.49	0.75	0.23	<0.0001
2	0.08	2.51	0.07	0.93	0.40

Data represent individual observations from six individuals for steady swimming, small turns and large turns. Discriminant power refers to the ability of the analysis to separate groups based on the contributing variables to a given discriminant axis. An axis significantly contributes to maximum linear separation of groups when $P<0.05$.

±0.62 cm s^{-1}, triple the average wave speed for steady swimming; therefore, the means differed significantly (Bonferroni; $t_5=-4.96$, $P=0.01$; Table 1).

Canonical discriminant analysis

The first canonical axis had 97.49% discriminating power and therefore was the axis significantly contributing to the maximum separation of steady swimming, small turns and large turns ($P<0.05$; Table 2, Fig. 6). Ribbon fin wavelength, wave speed, ribbon fin frequency, pectoral fin flapping frequency, maximum yaw angle and β_b positively correlated with the first discriminant axis (Fig. 6). AI, ribbon fin amplitude and pitch angle correlated negatively with the first axis (Fig. 6). Ribbon fin wavelength, wave speed and amplitude as well as maximum yaw angle were positively correlated with the second discriminant axis while the AI, pitch angle, pectoral fin frequency and β_b correlated negatively (Fig. 6). For the first canonical axis, β_b, ribbon fin frequency, ribbon fin wavelength and ribbon fin wave speed significantly contributed to the separation of treatments (Table S4). For the second canonical axis, pitch angle, β_b, ribbon fin frequency, ribbon fin wavelength and ribbon fin wave speed significantly contributed to the separation of treatments (Table S4).

Particle image velocimetry

In steady swimming sequences, we observed pairs of small counter-rotating vortices (0.17±0.036 mm^2) generated by the undulating ribbon fin (Fig. 7A; Table S5). In the sequences for small turns, we found that the paired vortices still occurred, but the magnitude of these vortices had increased towards the center of the ribbon fin during the turn (Fig. 7B; Table S5). The largest vortex pairs were observed in the large turn treatment (Fig. 7C; Table S5). Vortices formed during large turns (0.32–0.92 mm^2) were 190% larger than those formed during steady swimming (0.1–0.23 mm^2). Vortices produced during small turns (0.18–0.65 mm^2) were 84% larger than those formed during steady swimming and 58% smaller than vortices formed during large turns. To further illustrate the hydrodynamics during turning, velocity profiles for each treatment can be found in Fig. S1.

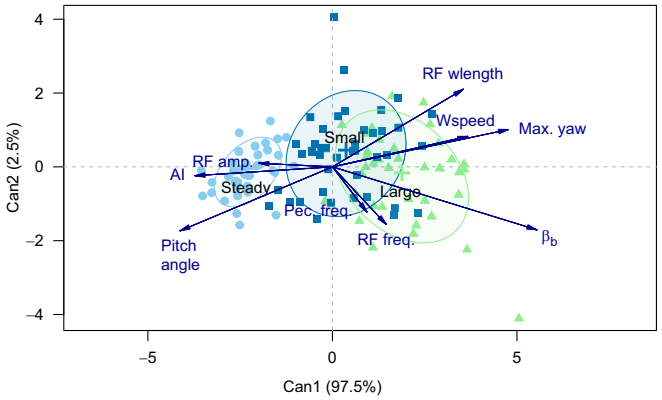

Fig. 6. Canonical discriminant analysis (CDA) for steady swimming, small turns and large turns. Canonical scores are represented by light blue circles for steady swimming, dark blue squares for small turns and green triangles for large turns. Crosses represent canonical means, and are surrounded by 68% probability ellipses. Kinematic variables included in the analysis were pitch angle (Pitch), body bending coefficient (β_b), maximum yaw angle (Max. yaw), asynchronous index (AI), pectoral flapping frequency (Pec. freq.), ribbon fin amplitude (RF amp.), ribbon fin wavelength (RF wlength), ribbon fin frequency (RF freq.) and wave speed (Wspeed).

DISCUSSION

Turning maneuvers in fishes are critical for survival and are involved in foraging, mating and habitat navigation. Most investigations of turning in fishes focus on species with traditional control surfaces, while the mechanisms of turning in those with non-traditional control surfaces have been largely overlooked. To add to our understanding of turning in fishes with non-traditional control surfaces, we investigated how the gymnotiform swimmer *A. albifrons* performs turning maneuvers using 3D kinematics and descriptive DPIV. Of the three control surfaces investigated (body, pectoral fins and ribbon fin), we expected that the ribbon fin would contribute most to steady swimming, the pectoral fins would dominate during small turns, and all three control surfaces would be employed during large turns. We found that during steady swimming and turning maneuvers, *A. albifrons* recruited all three control surfaces, to differing degrees. Hydrodynamically, large turns are associated with an increase in vortex magnitude.

During steady swimming, individuals held their body in a slight head-up orientation, also noted previously in studies investigating forward swimming in *A. albifrons* (Ruiz-Torres et al., 2013; Youngerman et al., 2014; Ortega-Jimenez and Sanford, 2021). It has been suggested that positive pitch angles while swimming may be an effect of upward forces generated by the undulating ribbon fin (Ruiz-Torres et al., 2013). As the ribbon fin undulates during swimming, counter-rotating vortices shed from the fin, causing downward momentum and a resulting heave force upwards (Shirgaonkar et al., 2008; Curet et al., 2010). In the absence of additional control surfaces, *A. albifrons* may use the pectoral fins to mitigate body instability caused by heave forces. The AI during steady swimming was significantly higher than the AI during large turns and indicated that ∼50% of the time the fins were used asynchronously during steady swimming (Table 1, Fig. 4C). Despite differences in AI, pectoral flapping frequency and pectoral dorso-ventral angle did not differ between steady swimming and the turning maneuvers (Table 1, Fig. 4A,B). In another ribbon fin swimmer, *Amia calva*, pectoral fin movements did not impact forward swimming speed, and it was suggested that pectoral movement may counterbalance the rotation around the fish's center of mass (Jagnandan and Sanford, 2013). It is possible that *A. albifrons* uses pectoral fins for stabilization rather than thrust generation during forward swimming, similar to *A. calva*.

With the pectoral fins used for stabilization, the ribbon fin is thought to be the main contributor to forward swimming (Ortega-

Journal of Experimental Biology (2022) 225, jeb243498. doi:10.1242/jeb.243498

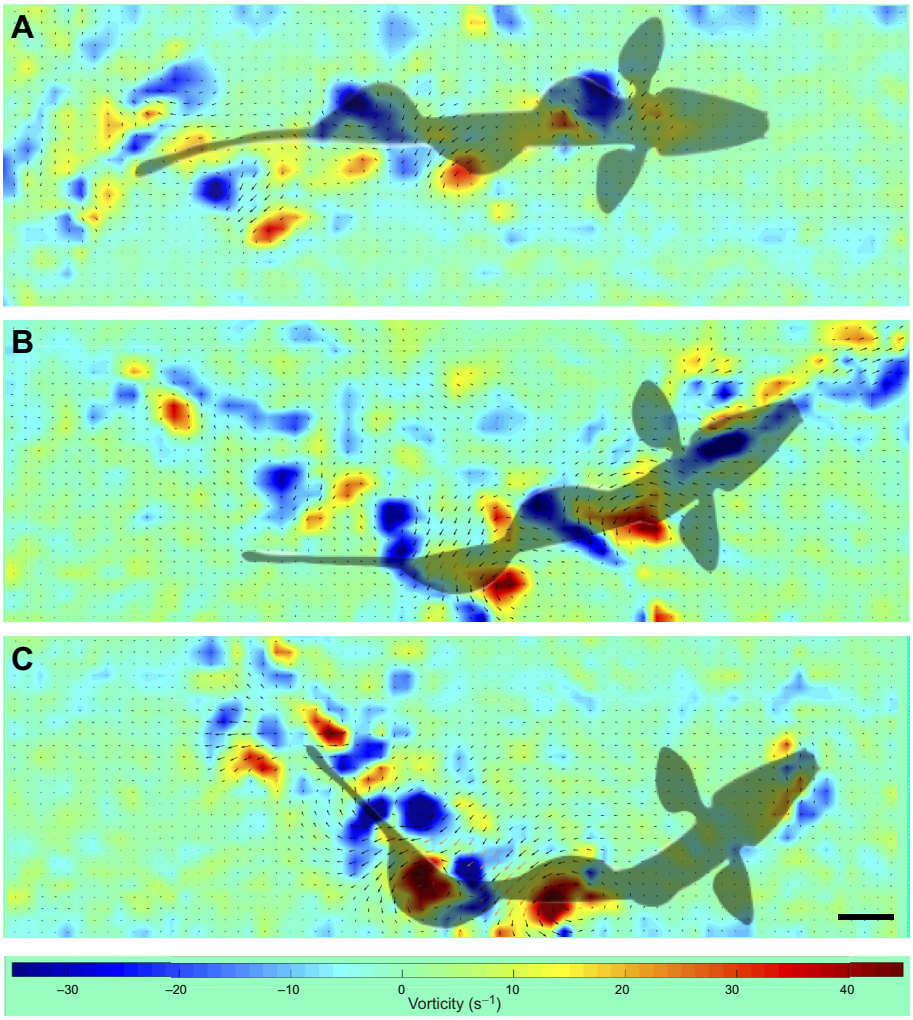

Fig. 7. Fluid dynamics of the ribbon fin during steady swimming and turning maneuvers. Vorticity fields representing steady swimming (A), small turn (B) and large turn treatments (C). Fish silhouettes show the relative location of the fish with the ribbon fin intersecting the laser sheet. Scale bar: 1 cm.

Jimenez and Sanford, 2021). Ribbon fin frequency, wavelength and wave speed were lowest during steady swimming while ribbon fin amplitude was slightly larger although not significantly different from that in turning treatments (Table 1, Fig. 5). According to Youngerman et al. (2014), ribbon fin frequency during forward swimming is generally 4–6 Hz, which is also reflected in our data (Table 1). Previous studies suggest modulation of frequency influences forward swimming speed, and this is one of the variables that significantly contributed to separating the treatments in the discriminant analysis (Jagnandan and Sanford, 2013; Youngerman et al., 2014; Ortega-Jimenez and Sanford, 2021) (Table S4).

The body exhibited significantly more bending during the small and large turns when compared with steady swimming (Table 1). In addition, significantly higher maximum yaw angles were observed during turning (Table 1, Fig. 3B,C). Studies of *A. albifrons* suggest turning maneuvers in this species are rare and body bending is not common (Blake, 1983; MacIver et al., 2001, 2010). However, in this study, *A. albifrons* clearly bent their bodies to follow an oscillating feeder and Youngerman et al. (2014) observed body bending during free swimming maneuvers. These results also follow the observations of Ortega-Jimenez and Sanford (2021) in which *A. albifrons* bent its body in response to swimming downstream from an oscillating cylinder. Furthermore, Kasapi et al. (1993) also observed that body bending contributed to escape maneuvers in the African knifefish (*Xenomystus nigri*), which also swims using the gymnotiform mode. Given the frequency of turning in this study and in lab observations of *A. albifrons*, body bending appears to be common despite any potential negative impacts on the electro–sensory system. In this species, electro-receptors are located around the head, and dorsal and lateral surfaces to allow the fish to easily detect prey upstream (Nelson and MacIver, 1999). During foraging observations, and during turning maneuvers in this study, *A. albifrons* navigated with a head-down (negative pitch) orientation (Nelson and MacIver, 1999). Maneuvering with a negative pitch angle may be not only behavioral but also a consequence of altering pectoral fin use to counter heave forces.

During small and large turns, there was no difference in flapping frequency or dorso-ventral abduction angle, but there was a difference in AI. While pectoral fin use can be considered asynchronous in all three treatments, asynchronous fin use occurred ∼30% of the time on average throughout large turns, ∼38% during small turns and ∼48% during steady swimming (Table 1, Fig. 4C). We did not expect pectoral fin asynchrony to be lower during turning maneuvers when compared with forward swimming, but we have presented an alternative metric for asynchrony in this study (AI). Ortega-Jimenez and Sanford (2021) quantified fin asymmetry angles as a means of understanding asynchronous fin use, and these angles were highest when *A. albifrons* followed an oscillating cylinder. However, as AI considers timing of the maneuver in its

calculation, it gives a glimpse of the temporal component of pectoral fin use. For instance, during turning, the inside fin initiated directional change, but through the remainder of the turn, the two fins were held in similar positions (Movie 1). Similarly, synchronous pectoral fin excursions were used to help power escape maneuvers in *X. nigri* (Kasapi et al., 1993). Synchronous pectoral fin movements may be used in tandem with acceleration of the ribbon fin to power turns, but we are restricted with our interpretation here as we did not measure acceleration in this study. However, Ortega-Jimenez and Sanford (2021) measured ribbon fin acceleration across different flow regimes, and considering the same flow speed (1.8 BL s^{-1}), acceleration increased from 45 cm s^{-1} in laminar flow to 484 cm s^{-1} when the fish actively followed an oscillating cylinder.

Ribbon fin wavelength was similar between small and large turns and contributed significantly to turning (Table 1, Fig. 5B; Table S3). As it is suggested that *A. albifrons* has active control over fin ray curvature, and larger wavelengths increase the surface area of the fin for fluid loading, active modulation of the ribbon fin appears to drive turning (Youngerman et al., 2014). Ribbon fin wave speed may also contribute to the amount of thrust that can be generated from fluid loading, which was supported by the observation that large turns were characterized by a significant increase in wave speed (Table 1, Fig. 5D). As previously mentioned, the ribbon fin generates heave forces which may grow in magnitude as wave speed increases, thus contributing to torque around the fish's center of mass, which would explain the negative pitch angle observed during turning (Fig. 3A).

In addition to the kinematic analysis, the hydrodynamic analysis suggests the ribbon fin is a major contributor to turning maneuvers. We observed that vortex size greatly increases from small turns to large turns, and previous analysis of the ribbon fin wake as *A. albifrons* followed an oscillating cylinder showed similar patterns (Fig. 7) (Ortega-Jimenez and Sanford, 2021). It is unclear whether instantaneous increases in wave speed during turning would result in higher energetic costs as it is not known whether the whole fin is under active or passive control. Understanding the extent to which *A. albifrons* controls different parts of the fin will increase our current understanding of the potential metabolic costs of gymnotiform swimming. It should be noted that our DPIV measurements only take into account the contribution of the ribbon fin. Previous work on knifefish swimming in perturbed flows suggests that the ribbon fin has a major contribution to thrust production, while the pectoral fins are used for swimming control (Ortega-Jimenez and Sanford, 2021). Future work that includes the hydrodynamics of the pectoral fins will provide a more complete understanding of their role in turning performance.

In the broader context of fish evolution, this study highlights the need to expand our knowledge of the contribution of alternative control surfaces to ecologically relevant maneuvers such as turning. Specifically, future studies would benefit from the investigation of other ribbon fin swimmers where the anatomical placement and morphology of the ribbon fin differs from that of *A. albifrons*, to gain a more comprehensive understanding of selective pressures associated with ribbon fin swimming. Beyond biology, the results of these types of investigations can be applied to current models of ribbon fin inspired AUVs (MacIver et al., 2004; Curet et al., 2011; Neveln et al., 2013). In the case of *A. albifrons* and other gymnotid knifefishes in the Amazon that are facing increasingly unpredictable water levels in their habitats, understanding maneuvering performance may inform ecologists of the potential spatial constraints on these species. In structurally complex habitats such as the Amazon, low water (decreased volume) regimes reduce the amount of open space for navigation in between flood plains and river systems, which may hinder foraging, mating and seasonal migrations in certain fish assemblages (Fernandes, 1997; Silva et al., 2021).

In conclusion, we highlight the important contribution of a non-traditional control surface to turning maneuvers in a gymnotiform swimmer. The kinematics data suggest that the ribbon fin is recruited heavily during turning, with body bending and pectoral fin movements contributing to changes in heading and stabilization. Our descriptive hydrodynamics data show that vortices during turning are larger than those during steady swimming. Future studies should investigate maneuvering in other ribbon fin swimmers to further understand the convergence of this swimming mode, inspire more maneuverable AUVs and further understand the ecomorphological implications of the ribbon fin.

Acknowledgements
The authors would like to thank Dante Orlando for assistance in building and programming the oscillating feeder and Ashlyn Stanalonis for help with filming and fish care. The authors also thank two anonymous reviewers for their insightful comments on the manuscript.

Competing interests
The authors declare no competing or financial interests.

Author contributions
Conceptualization: O.H.H., V.M.O., C.P.S.; Methodology: O.H.H., V.M.O., C.P.S.; Software: V.M.O.; Validation: O.H.H., V.M.O.; Formal analysis: O.H.H.; Investigation: O.H.H.; Resources: C.P.S.; Data curation: O.H.H., V.M.O.; Writing - original draft: O.H.H.; Writing - review & editing: V.M.O., C.P.S.; Visualization: O.H.H.; Supervision: V.M.O., C.P.S.; Project administration: C.P.S.; Funding acquisition: C.P.S.

Funding
This work was supported by the College of Science and Mathematics at Kennesaw State University [C.P.S.].

Data availability
Code for digitization used in this study is available at: https://biomech.web.unc.edu/dltdv/. Code supporting DPIV analysis can be found at: https://pivlab.blogspot.com/2017/07/pivlab-direct-download.html. Datasets are available from the Dryad digital repository (Hawkins et al., 2022): https://doi.org/10.5061/dryad.9ghx3ffhj

References
Albert, J. S. (2001). Species diversity and phylogenetic systematics of American knifefishes (Gymnotiformes, Teleostei). *Misc. Publ. Mus. Zool. Univ. Michigan* **190**, 1-127.

Albert, J. S. and Crampton, W. G. R. (2005). Diversity and phylogeny of Neotropical electric fishes (Gymnotiformes). In *Electroreception* (ed. R. R. Fay, A. N. Popper, T.H. Bullock and C. D. Hopkins), pp. 360-409. Springer Handbook of Auditory Research, Vol. 21. New York: Springer Publishing.

Azizi, E. and Landberg, T. (2002). Effects of metamorphosis on the aquatic escape response of the two-lined salamander (*Eurycea bislineata*). *J. Exp. Biol.* **205**, 841-849. doi:10.1242/jeb.205.6.841

Blake, R. W. (1983). Swimming in the electric eels and knifefishes. *Can. J. Zool.* **61**, 1432-1441. doi:10.1139/z83-192

Budick, S. A. and O'Malley, D. M. (2000). Locomotor repertoire of the larval zebrafish: swimming, turning and prey capture. *J. Exp. Biol.* **203**, 2565-2579. doi:10.1242/jeb.203.17.2565

Crampton, W. G. R. (1996). Gymnotiform fish: an important component of Amazonian floodplain fish communities. *J. Fish. Biol.* **48**, 298-301. doi:10.1006/jfbi.1996.0029

Curet, O. M., AlAli, I. K., MacIver, M. A. and Patankar, N. A. (2010). A versatile implicit iterative approach for fully resolved simulation of self-propulsion. *Comput. Methods Appl. Mech. Eng.* **199**, 2417-2424. doi:10.1016/j.cma.2010.03.026

Curet, O. M., Patankar, N. A., Lauder, G. V. and MacIver, M. A. (2011). Aquatic maneuvering with counter-propagating waves: a novel locomotive strategy. *J. R. Soc. Interface.* **8**, 1041-1050. doi:10.1098/rsif.2010.0493

Domenici, P. (2001). The scaling of locomotor performance in predator-prey encounters: from fish to killer whales. *Comp. Biochem. Physiol. A* **131**, 169-182. doi:10.1016/S1095-6433(01)00465-2

Domenici, P., Standen, E. M. and Levine, R. P. (2004). Escape manoeuvres in the spiny dogfish (*Squalus acanthias*). *J. Exp. Biol.* **207**, 2339-2349. doi:10.1242/jeb.01015

Drucker, E. and Lauder, G. (2001). Wake dynamics and fluid forces of turning maneuvers in sunfish. *J. Exp. Biol.* **204**, 431-442. doi:10.1242/jeb.204.3.431

Drucker, E. G. and Lauder, G. V. (2002). Wake dynamics and locomotor function in fishes: interpreting evolutionary patterns in pectoral fin design. *Intgr. Comp. Biol.* **42**, 997-1008. doi:10.1093/icb/42.5.997

Ellerby, D. J. and Gerry, S. P. (2011). Sympatric divergence and performance trade-offs of bluegill ecomorphs. *Evol. Biol.* **38**, 422-433. doi:10.1007/s11692-011-9130-y

English, I., Liu, H. and Curet, O. M. (2019). Robotic device shows lack of momentum enhancement for gymnotiform swimmers. *Bioinspir. Biomim.* **14**, p.aaf983. doi:10.1088/1748-3190/aaf983.

Feng, Y. K., Liu, H. X., Su, Y. Y. and Su, Y. M. (2020). Numerical study on the hydrodynamics of C-turn maneuvering of a tuna-like fish body under self-propulsion. *J. Fluids Struct.* **94**, 102954. doi:10.1016/j.jfluidstructs.2020.102954

Fernandes, C. C. (1997). Lateral migration of fishes in Amazon floodplains. *Ecol. Fresh. Fish* **6**, 36-44. doi:10.1111/j.1600-0633.1997.tb00140.x

Flammang, B. E. and Lauder, G. V. (2013). Pectoral fins aid in navigation of a complex environment by Bluegill Sunfish Under Sensory Deprivation Conditions. *J. Exp. Biol.* **216**, 3084-3089. doi:10.1242/jeb.080077

Gerry, S. P., Ramsay, J. B., Dean, M. N. and Wilga, C. D. (2008). Evolution of asynchronous motor activity in paired muscles: effects of ecology, morphology, and phylogeny. *Integr. Comp. Biol.* **48**, 272-282. doi:10.1093/icb/icn055

Gerstner, C. L. (1999). Maneuverability of four species of coral-reef fish that differ in body and pectoral fin morphology. *Can. J. Zoo.* **77**, 1102-1110. doi:10.1139/z99-086

Gibb, A. C., Swanson, B. O., Wesp, H., Landels, C. and Liu, C. (2006). Development of the escape response in teleost fishes: do ontogenetic changes enable improved performance? *Physiol. Biochem. Zool.* **79**, 7-19. doi:10.1086/498192

Hawkins, O., Ortega-Jimenez, V. and Sanford, C. (2022). Knifefish turning control and hydrodynamics during forward swimming. *Dryad Dataset*. doi:10.5061/dryad.9ghx3ffhj

Hedrick, T. L. (2008). Software techniques for two- and three-dimensional kinematic measurements of biological and biomimetic systems. *Bioinsp. Biomim.* **3**, 034001. doi:10.1088/1748-3182/3/3/034001

Jagnandan, K. and Sanford, C. P. (2013). Kinematics of ribbon-fin locomotion in the bowfin, *Amia calva*. *J. Exp. Zool. A.* **319**, 569-583. doi:10.1002/jez.1819

Kasapi, M. A., Domenici, P. D., Blake, R. W. and Harper, D. G. (1993). The kinematics and performance of escape responses of the knifefish *Xenomystus nigri*. *Can. J. Zool.* **71**, 189-195. doi:10.1139/z93-026

Katz, E., Lammel, A. and Bonnet, M. P. (2020). Climate change in a floodplain of the Brazilian Amazon: scientific observation and local knowledge. In *Changing Climate, Changing Worlds* (ed. M. Welch-Devine, A. Sourdril and B. Burke), pp. 123-144. Ethnobiology. Cham: Springer. doi:10.1007/978-3-030-37312-2_7

Lauder, G. V. and Drucker, E. G. (2004). Morphology and experimental hydrodynamics of fish fin control surfaces. *IEEE J. Ocean. Eng.* **29**, 556-571. doi:10.1109/JOE.2004.833219

Li, X. (2021). Hydrodynamic analysis for the morphing median fins of tuna during Yaw Motions. *App. Bionics Biomech* **2021**, 6630839. doi:10.1155/2021/6630839

Liotta, M. N., Abbott, J. K., Rios-Cardenas, O. and Morris, M. R. (2019). Tactical dimorphism: the interplay between body shape and mating behaviour in the swordtail *Xiphophorus multilineatus* (Cyprinodontiformes: Poeciliidae). *Biol. J. Linn. Soc.* **127**, 337-350. doi:10.1093/biolinnean/blz053

Liu, H. and Curet, O. M. (2018). Swimming performance of a bio-inspired robotic vessel with undulating fin propulsion. *Bioinsp. Biomim.* **13**, 056006. doi:10.1088/1748-3190/aacd26

MacIver, M. A., Sharabash, N. M. and Nelson, M. E. (2001). Prey-capture behavior in gymnotid electric fish: motion analysis and effects of water conductivity. *J. Exp. Biol.* **204**, 543-557. doi:10.1242/jeb.204.3.543

MacIver, M. A., Fontaine, E. and Burdick, J. W. (2004). Designing future underwater vehicles: principles and mechanisms of the weakly electric fish. *IEEE J. Oceanic Eng.* **29**, 651-659. doi:10.1109/JOE.2004.833210

MacIver, M. A., Patankar, N. A. and Shirgaonkar, A. A. (2010). Energy-information trade-offs between movement and sensing. *PLoS Comput. Biol.* **6**, e1000769. doi:10.1371/journal.pcbi.1000769

Moyer, J. T. (1979). Mating strategies and reproductive behaviour of ostraciid fishes at Miyake-Jima, Japan. *Jap. J. Ichthyol.* **26**, 148-160.

Nelson, M. E. and MacIver, M. A. (1999). Prey capture in the weakly electric fish *Apteronotus albifrons*: sensory acquisition strategies and electrosensory consequences. *J. Exp. Biol.* **202**, 1195-1203. doi:10.1242/jeb.202.10.1195

Neveln, I. D., Bai, Y., Snyder, J. B., Solberg, J. R., Curet, O. M., Lynch, K. M. and MacIver, M. A. (2013). Biomimetic and bio-inspired robotics in electric fish research. *J. Exp. Biol.* **216**, 2501-2514. doi:10.1242/jeb.082743

Ortega-Jimenez, V. M. and Sanford, C. P. (2021). Beyond the Kármán Gait: Knifefish swimming in periodic and irregular vortex streets. *J. Exp. Biol.* **224**, jeb238808. doi:10.5061/dryad.sqv9s4n37

Pavlov, V., Rosental, B., Hansen, N. F., Beers, J. M. and Parish, G. (2017). Hydraulic control of tuna fins: A role for the lymphatic system in vertebrate locomotion. *Science.* **357**, 310-314. doi:10.1126/science.aak9607

Ruiz-Torres, R., Curet, O. M., Lauder, G. V. and MacIver, M. A. (2013). Kinematics of the ribbon fin in hovering and swimming of the electric ghost knifefish. *J. Exp. Biol.* **216**, 823-834. doi:10.1242/jeb.076471

Shirgaonkar, A. A., Curet, O. M., Patankar, N. A. and MacIver, M. A. (2008). The hydrodynamics of ribbon-fin propulsion during impulsive motion. *J. Exp. Biol.* **211**, 3490-3503. doi:10.1242/jeb.019224

Silva, P. B., Arantes, C. C., Freitas, C. E. C., Petrere, M. and Ribeiro, F. R. V. (2021). Seasonal hydrology and fish assemblage structure in the floodplain of the lower Amazon River. *Ecol. Freshw. Fish.* **30**, 162-173. doi:10.1111/eff.12572

Standen, E. M. (2008). Pelvic fin locomotor function in fishes: three-dimensional kinematics in rainbow trout (*Oncorhynchus mykiss*). *J. Exp. Biol.* **211**, 2931-2942. doi:10.1242/jeb.018572

Standen, E. M. and Lauder, G. V. (2005). Dorsal and anal fin function in bluegill sunfish *Lepomis Macrochirus*: three-dimensional kinematics during propulsion and maneuvering. *J. Exp. Biol.* **208**, 2753-2763. doi:10.1242/jeb.01706

Standen, E. M. and Lauder, G. V. (2007). Hydrodynamic function of dorsal and anal fins in Brook Trout (*Salvelinus Fontinalis*). *J. Exp. Biol.* **210**, 325-339. doi:10.1242/jeb.02661

Thielicke, W. and Stamhuis, E. J. (2014). PIVlab – towards user-friendly, affordable and accurate digital particle image velocimetry in MATLAB. *J. Open Res. Soft.* **2**, e30. doi:10.5334/jors.bl

Tytell, E. D. and Lauder, G. V. (2002). The C-start escape response of *Polypterus senegalus*: bilateral muscle activity and variation during stage 1 and 2. *J. Exp. Biol.* **205**, 2591-2603. doi:10.1242/jeb.205.17.2591

Tytell, E. D. and Lauder, G. V. (2008). Hydrodynamics of the escape response in bluegill sunfish, *Lepomis macrochirus*. *J. Exp. Biol.* **211**, 3359-3369. doi:10.1242/jeb.020917

von der Emde, G. and Bleckmann, H. (1998). Finding food: senses involved in foraging for insect larvae in the electric fish *Gnathonemus petersii*. *J. Exp. Biol.* **7**, 969-980. doi:10.1242/jeb.201.7.969

Walker, J. A. (1998). Estimating velocities and accelerations of animal locomotion: a simulation experiment comparing numerical differentiation algorithms. *J. Exp. Biol.* **201**, 981-995. doi:10.1242/jeb.201.7.981

Walker, J. A. (2000). Does a rigid body limit maneuverability? *J. Exp. Biol.* **203**, 3391-3396. doi:10.1242/jeb.203.22.3391

Webb, P. W. (1976). The effect of size on the fast-start performance of rainbow trout *Salmo gairdneri* and a consideration of piscivorous predator-prey interaction. *J. Exp. Biol.* **65**, 157-177. doi:10.1242/jeb.65.1.157

Webb, P. W. (1978). Fast-start performance and body form in seven species of teleost fish. *J. Exp. Biol.* **74**, 211-226. doi:10.1242/jeb.74.1.211

Webb, P. W. (1981). Composition and mechanics of routine swimming of rainbow trout, *Oncorhynchus mykiss*. *Can. J. Fish. Aquat. Sci.* **48**, 583-590. doi:10.1139/f91-074

Weihs, D. (1972). A hydrodynamical analysis of fish turning maneuvers. *Proc. R. Soc. B.* **182**, 69-72. doi:10.1098/rspb.1972.0066

Wöhl, S. and Schuster, S. (2007). The predictive start of hunting archer fish: a flexible and precise motor pattern performed with the kinematics of an escape C-start. *J. Exp. Biol.* **210**, 311-324. doi:10.1242/jeb.02646

Youngerman, E. D., Flammang, B. E. and Lauder, G. V. (2014). Locomotion of free-swimming ghost knifefish: anal fin kinematics during four behaviors. *Zool.* **117**, 337-348. doi:10.1016/j.zool.2014.04.004

Zin, M. A. M., Rambely, A. S., Ariff, N. M. and Ariffin, M. S. (2020). Smoothing and differentiation of kinematic data using functional data analysis approach: an application of automatic and subjective methods. *Appl. Sci.* **10**, 2493. doi:10.3390/app10072493